Earth and Planetary Science Letters 308 (2011) 433–444

Contents lists available at ScienceDirect

Earth and Planetary Science Letters

journal homepage: www.elsevier.com/locate/epsl

New Arabian Sea records help decipher orbital timing of Indo-Asian monsoon

Thibaut Caley [a,*], Bruno Malaizé [a], Sébastien Zaragosi [a], Linda Rossignol [a], Julien Bourget [b], Frédérique Eynaud [a], Philippe Martinez [a], Jacques Giraudeau [a], Karine Charlier [a], Nadine Ellouz-Zimmermann [c]

[a] Université de Bordeaux, UB1, CNRS, UMR 5805 EPOC, France
[b] Australian School of Petroleum, Centre for Tectonics, Resources and Exploration (TRaX), The University of Adelaide, Adelaide 5005, Australia
[c] IFP, Geology-Geochemistry-Geophysics, 1 & 4 avenue de Bois Préau, F-92852 Rueil-Malmaison, France

ARTICLE INFO

Article history:
Received 3 March 2011
Received in revised form 9 June 2011
Accepted 20 June 2011
Available online 13 July 2011

Editor: P. DeMenocal

Keywords:
summer/winter monsoon
productivity
Arabian Sea
timing
precession
obliquity

ABSTRACT

A recent study suggested that Indian monsoonal proxies commonly used in the Arabian Sea, in general productivity proxies, could be impacted by changes in the Atlantic overturning rate (AMOC) throughout a control on the nutrient delivery into the euphotic zone. This oceanic mechanism could lead to a misunderstanding between the Indian summer monsoon (SM) and orbital forcing and could confuse a direct comparison with other archives derived from other monsoonal sub-systems (such as East-Asian or African records). Here we analyze three independent proxies (bromine, foraminifera assemblages and grain size) extracted from a marine sediment core (MD04-2861) covering the last 310 ka, and retrieved in the northern Arabian Sea near the Makran margin, an area influenced by summer and winter Indian monsoon. The grain size proxy deals with the regional continental climate through fluvial and eolian processes. It cannot be linked to changes in nutrient content of AMOC and present the same phase relationship (timing) than the other SM proxies. This demonstrates that the productivity signals (Bromine) in the northern Arabian Sea are mainly controlled by SM dynamics and not AMOC modulated nutrients at orbital scale changes. We thus build a multi-proxy record of SM variability (i.e. SM stack) using statistical tools (principal component analysis) further compiled on an age model constructed independently from orbital tuning. We find that strong SM lag by 9 ± 1 ka the NH summer insolation maximum (minimum of precession, June 21 perihelion and obliquity maximum) in the precession band, and by 6 ± 1.3 ka in the Obliquity band. These results are consistent with previous studies based on marine and terrestrial records in both Indian and Asian regions, except Asian speleothems. Our study supports the hypothesis that internal climate forcing (decreased ice volume together with the increase of latent heat export from the southern Indian Ocean) set the timing of strong Indo-Asian summer monsoons within both the precession and obliquity cycle. The external forcing (direct sensible heating) initiate monsoonal circulation. Strong Indian winter monsoon (WM) occurs between ice maxima and northern hemisphere sensible heat minima, indicating that both act to strengthen WM circulation. The summer and winter monsoons are in antiphase in the precession band suggesting that the two systems are dynamically linked.

1. Introduction

The Indo-Asian monsoon represents the strongest expression of the monsoon modern dynamics, allowing important transfers of moisture at a large geographical scale and deeply affecting human populations. Monsoon strength and variability is crucial for the economical prosperity of regions.

The forcing/response relationship of the Indo-Asian monsoon at orbital scale during the Quaternary period is still debated in the literature. This lack of understanding how of the monsoon responds to the most fundamental of boundary conditions at this time scale (insolation, ice-volume, greenhouse gasses, ocean–atmosphere energy exchange) does not bode well for predicting monsoon response to future climate change. Two different hypotheses exist and are based upon observed timing.

(1) Clemens and Prell (2003) and Clemens et al. (2008, 2010) focussed their studies on wind-derived proxies within sedimentological archives from the Owen Ridge, northern Arabian Sea. They proposed that strong events of Indo-Asian summer monsoon lag by ~8 ka the maximum northern hemisphere (NH) summer insolation (minimum of precession, June 21 perihelion).
(2) From the analysis of Chinese cave speleothems (Cheng et al., 2009; Dykoski et al., 2005; Wang et al., 2001; 2008), a shorter lag of only ~3 ka was observed between strong summer monsoon and maximum NH summer insolation.

* Corresponding author. Tel.: +33 5 40 00 83 81; fax: +33 5 56 84 08 48.
E-mail address: t.caley@epoc.u-bordeaux1.fr (T. Caley).

0012-821X/$ – see front matter © 2011 Elsevier B.V. All rights reserved.
doi:10.1016/j.epsl.2011.06.019

The recent study of Ziegler et al. (2010a) conducted in the Arabian Sea proposed that the summer monsoonal proxies, in general productivity-based proxies, could be influenced by other processes not only related to monsoon forcing. This recent study casts some doubt on the interpretation of the 8 ka lag between precession minima and strong summer monsoons as driven by latent heat export from the southern hemisphere (Ziegler et al., 2010a–b). Indeed, Ziegler et al. (2010a) have proposed that biological productivity and OMZ intensity at the precession frequency band are mainly controlled by changes in the intensity of the Atlantic meridional overturning circulation (AMOC) which controlled the nutrient delivery in the euphotic zone of the Arabian Sea.

The aim of our study is to carry new insights about Indo-Asian monsoon forcing and response (phase relationship). We used a sedimentary core located in the northern Arabian Sea, close to the Makran margin. To complete previous works which generally focus their interpretations on the monsoon processes with productivity-based proxies, we have analyzed tools linked to productivity, but also foraminifera assemblages together with grain size parameters dealing with the regional continental climate. Based on our new results and the comparisons with previous published data, we discuss the orbital forcing and response of the Indo-Asian monsoon system.

2. Environmental setting

The studied core MD04-2861 is located in the Arabian Sea, off the tectonically-active Makran margin (24.13 N; 63.91 E; 2049 m depth) (Bourget et al., 2011; Ellouz-Zimmermann et al., 2007; Kukowski et al., 2001; Fig. 1A). This core was retrieved on the little Murray Ridge, northward of the Murray Ridge where Ziegler et al. (2010a) have studied cores NIOP463 and MD04-2876. Sites investigated by Clemens and Prell (2003) are located southward in the Arabian Sea, on the Owen Ridge (Fig. 1A).

Nowadays, Arabian Sea environments experience large seasonal variations due to strong monsoonal winds and associated migration of the InterTropical Convergence Zone (ITCZ) (Clemens and Prell, 2003; Luckge et al., 2001; Sirocko et al., 1991; von Rad et al., 1995). The seasonal reversal in the wind direction is also associated with contrasted precipitations, high variability in the sediment inputs and drastic changes in oceanic current strength and direction (Schott et al., 2009; Sirocko et al., 2000; von Rad et al., 1999). During the summer season (SW monsoon) (Fig. 1B), warmer and more humid conditions are observed over Karachi and the Indian subcontinent (Luckge et al., 2001). During the winter season (NE monsoon), precipitations also occur (Luckge et al., 2001) linked to the cyclonic low-pressure systems originating in the eastern Mediterranean which occasionally penetrate the Arabian landmass (Weyhenmeyer et al., 2000). However, arid conditions generally dominate during the winter monsoon, and paleostudies suggest that the origin of atmospheric water vapor changed from a dominantly northern Mediterranean source (modern pattern), to a primarily southern Indian Ocean source during the Late Pleistocene (Weyhenmeyer et al., 2000). Even if the Pakistan region received less than 200 mm of annual precipitation today (Pakistan Meteorological Department), the climate of the region results in intense flash flooding of the drainage system over the Makran region linked to this continental humidity/aridity balance (von Rad et al., 1999). A large number of fluvial systems are distributed along the Makran coast (Fig. 1A) and are associated offshore with the presence of several submarine canyons along the Makran continental slope (Bourget et al., 2010; 2011). Turbidity current activity has been recorded in both slope and abyssal plain areas throughout the Pleistocene and the Holocene (Bourget et al., 2010; Prins and Postma, 2000). However, our core is located on a submarine topographic high, up to ~1000 m above the surrounding sea-floor, preventing our site from any direct influence of turbidity currents on the sedimentary processes. Meanwhile our coring site is located relatively close to the coast (less than 150 km) and thus could be influenced by sediment supply from the continent, via fluvial and/or aeolian transport and decantation in the water column. Regional dust transport (Sirocko et al., 2000), controlled by both continental aridity and wind strength, is likely to influence the sedimentation at our core site. The increase/decrease of wind allows the development/suppression of a strong coastal upwelling along the Oman margin, which adds a biogenic component to the lithogenic sedimentation (Clemens et al., 1996; Clemens and Prell, 1991; Reichart et al., 1998) (Fig. 1B). Large eddies and filaments generated during the SW monsoon upwelling (as visible at Ras al Hadd; Fig. 1B) are transported north-eastward to the Arabian Sea and affect our site (Fig. 1). Moderate NE wind blowing during the NE monsoon is also driving upwelling and enhanced productivity along the Makran coast (Fig. 1). Supply of oxygen-poor intermediate waters (You, 1998) combined with high surface productivity (linked to upwelling reinforcement) produce an intense oxygen minimum zone (OMZ). Our core site is located below the present day extension of this OMZ (Supplementary Fig. 1).

3. Material and methods

3.1. Bromine measurements

Bromine measurements were performed with an Avaatech XRF core scanner at EPOC laboratory. Each core section was scanned every 2 cm with ionization energy of 30 kv. Bromine counts are exclusively associated to marine organic content (MOContent) in the sediment of Arabian Sea (Ziegler et al., 2008). An increase in Bromine is associated to an increase in MOContent. Further information about the XRF scanning technique and its interest in paleostudies can be found in Richter et al. (2006).

3.2. Grain size analysis

Grain size analysis were performed using a Malvern™ Supersize 'S' at EPOC laboratory every 10 cm in the core. For some additional samples, we have removed carbonate prior to grain size analyses. Carbonate was removed using 20% Acetic Acid (48 h at room temperature).

3.3. Thin section

To obtain high-resolution sedimentological information in core MD04-2861, thin section was performed at EPOC laboratory using the method described in Zaragosi et al. (2006). We realized a thin section at 1930–1940 cm in core MD04-2861. Vertical cross-sections were made in the middle of the sediment/resin sample obtained using a diamond saw. Then, thin-section images were acquired using a fully automated Leica DM6000 B Digital Microscope using analyzed polarized light at EPOC laboratory.

3.4. Foraminifera assemblage

The subsamples were dried, weighed, and washed every 10 cm in the core through a 150 μm mesh sieve. Total assemblages of planktonic foraminifera were analyzed using an Olympus SZH10 binocular microscope following the taxonomy of Hemleben et al. (1989) and Kennett and Srinivasan (1983). About 300 specimens were counted in each level after splitting with an Otto microsplitter.

3.5. Isotopes

Specimens were picked within the 250–315 μm size fraction every 10–20 cm in the core. Benthic isotopic analyses were carried out on the species *Planulina wuellestorfi* at EPOC laboratory. Those solid, calcium carbonate samples (50 to 100 μg of foraminifer shells) were individually reacted with ortho-phosphoric acid to produce CO_2 gas, which was analyzed with an Optima© stable isotope mass

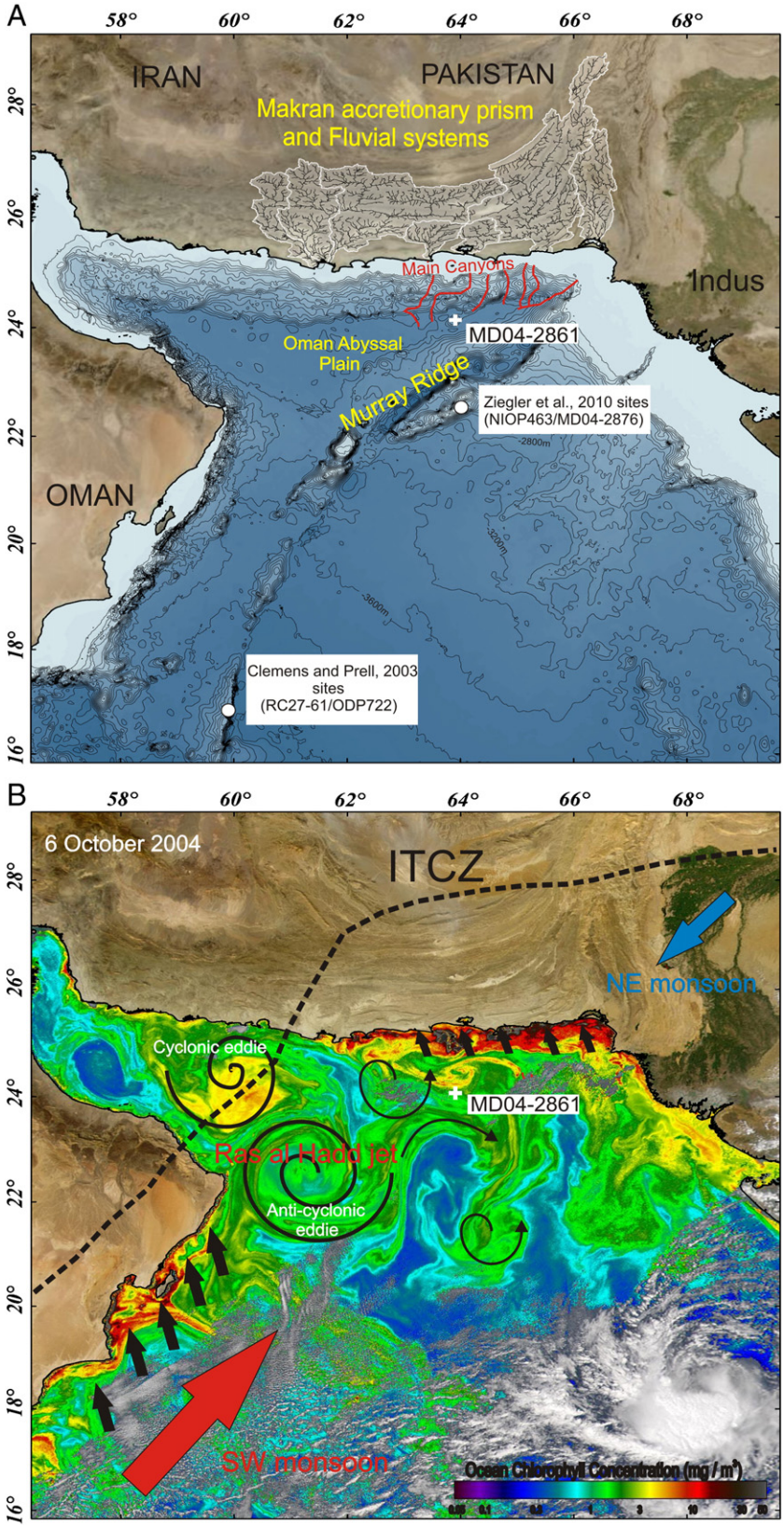

Fig. 1. Environmental setting for core MD04-2861. A) Location of the studied core close to the Makran accretionary prism and location of sites studied by Clemens and Prell (2003) and Ziegler et al. (2010a,b,c) (Bathymetry from http://www.gebco.net/). The main fluvial systems and canyons allowing important transfer of sediments are indicated. B) Important atmospheric and hydrologic processes for the Arabian Sea. Example of productivity (October) trough ocean chlorophyll concentration (SeaWIFS image from http://oceancolor.gsfc.nasa.gov/cgi/image_archive.cgi?c=CHLOROPHYLL). The presence of the summer upwelling is visible along the Oman (dark arrows) with important northward propagation of eddies and filaments (Ras al Hadd jet) towards site MD04-2861 during the strong SW monsoon. The position of the InterTropical Convergence Zone during summer season is indicated. Also visible is the development of the upwelling (dark arrows) along the Pakistan shelf during the moderate NE monsoon. Note that upwelling favorable winds (SW monsoon) typically set up in May (NCAR NCEP reanalysis data).

spectrometer against calibrated reference gas. $\delta^{18}O$ values are reported relative to Vienna PDB standard (VPDB) through calibrations to the international standard NBS19. External reproducibility is $\pm 0.05‰$ (1σ).

3.6. Spectral analysis and phase estimation

All the spectral analysis and phase estimation was performed with the Analyseries software (Paillard et al., 1996). Proxies have been spectrally compared with an astronomical index called ETP to evaluate coherence and phase (timing) relative to orbital extremes (Imbrie et al., 1984). ETP is constructed by normalizing and stacking Eccentricity, Tilt (obliquity) and negative Precession.

4. Results and discussion

4.1. Orbital and independent age model

Core stratigraphy for the upper part (~40 ka) has been established using 10 ^{14}C AMS dating from planktonic foraminifera species (Supplementary Table 1). Radiocarbon dates have been corrected for a marine reservoir effect of 400 years and calibrated to calendar years using CALIB Rev 5.0/Marine04 data set (Bard, 1998; Stuiver et al., 1998). Radiocarbon ages of this study were performed at the 'Laboratoire de Mesure du Carbone 14' in Saclay ('SacA') through the "ARTEMIS" radiocarbon dating project. All ages in the following text are given in calendar age (cal. BP).

Beyond the range of AMS ^{14}C ages, oxygen isotope stratigraphy has been applied for the entire core (Fig. 2 and supplementary Fig. 2). For that purpose, we correlate the $\delta^{18}O$ signal obtained on the benthic species (*P. wuellerstorfi*) with the "LR04" stack signal (Lisiecki and Raymo, 2005) using the Analyseries software (Paillard et al., 1996) (Fig. 2 and supplementary Fig. 2). This age model shows that the sedimentation rate in the core is relatively constant (Fig. 2).

Nevertheless, one of the goal of our study is to precisely document the timing (phases relative to orbital extremes) of Arabian Sea records to determine if our proxies are related to monsoonal forcing. The tuning done with the LR04 thus prevent us for independent analyses. In addition, benthic oxygen isotope signal in the Arabian Sea could be complicated by susceptibility to changes in carbonate ion concentration and supralysoclinal calcite dissolution (Schmiedl and Mackensen, 2006).

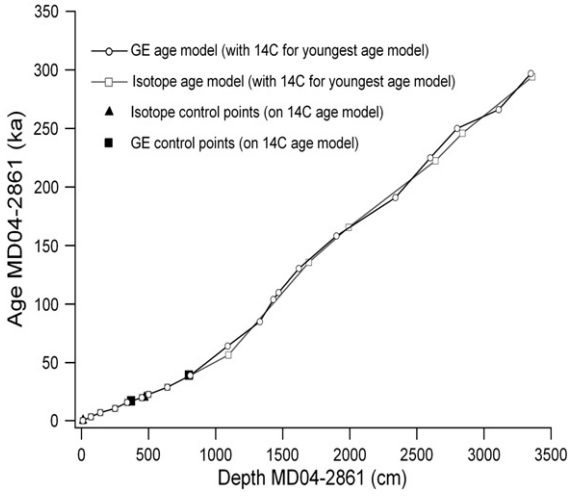

Fig. 2. Comparison of sedimentation rates calculated after two age models: the orbital age model (^{14}C and isotopes, (open squares)) and the age model (open circles) not relying upon orbital assumptions (^{14}C and GEs). The sedimentation rates are consistent between age models and relatively constant.

Therefore, we developed an alternative chronology based on a quantitative record of the planktonic foraminifera species *Globorotalia truncatulinoides* and *Globorotalia crassaformis* following previous studies in the area (Jaeschke et al., 2009; Ziegler et al., 2010a). During major cold events in the North Atlantic (Henrich events), high occurrences of these two deep-dwelling *Globorotalia* species were observed by Ziegler et al. (2010a). These *Globorotalia* events (GEs) coincided with a reduction or absence of the OMZ in the Arabian Sea as previously documented for HEs (Reichart et al., 1998; 2004). Ziegler et al. (2010a) refined their stratigraphy independently from orbital tuning by correlating GEs with the alkenone-derived SST long record obtained on the Iberian margin (Martrat et al., 2007) complemented by radioisotopic age constraints derived from U/Th dates on speleothem records (see Ziegler et al., 2010a,b,c for constraints sources). In our core, we observed 13 major GEs over the last 310 ka that we have correlated with the age constraint of Ziegler et al. (2010a) to build an age model not relying upon orbital assumptions (Table 1, Fig. 2 and supplementary Fig. 2). For GE 1 and 3 we kept the ^{14}C ages that appeared to be very consistent with the GEs ages from Ziegler et al. (2010a) (Table 1, Fig. 2). This "Independent" age model assumes that Arabian Sea GE events, North Atlantic 980 IRD events, Iberian Margin total alkenone events and speleothem events are temporally correlative at the orbital scale.

As long as the age model based on ^{14}C and GEs is coherent with the isotope stratigraphy (Table 1, Fig. 2, supplementary Table 2), we will use it in the following part of our study to precisely determine the forcing/response relationships of our records at orbital scale (see supplementary Table 2 for the effect of the two different age models on phase estimations for Arabian Sea records).

.

4.2. Foraminifera assemblage proxy

Thirty-seven species were identified in the fossil planktonic foraminifera assemblage from core MD04-2861. *G. bulloides*, *G. ruber* and *G. glutinata* are the most abundant species reaching 54% of the total assemblage. Also important are *O. universa*, *G. trilobus*, *G. sacculifer*, *G. calida*, *G. falconensis* and *N. pachyderma* (*dextral* coiling). These nine species represent up to 82% of the total assemblage.

Our core site is likely to be influenced by the regional SW (summer) and NE (winter) monsoon. According to Conan and Brummer (2000), *G. bulloides* and *G. glutinata* dominate the SW monsoon. Studies conducted on modern communities have demonstrated that these two species dwell preferentially in mixed and nutrient-rich waters (Conan and Brummer, 2000; Schiebel et al., 2001), a situation which occurs during the SW monsoon coastal upwelling development along the Oman and Somali margin. These species are also dominant in our

Table 1
Age constrains of GEs (ka) in core MD04-2861 and comparison with ^{14}C and isotopic stratigraphy.

Globorotalia events	Depht MD04-2861 (cm)	^{14}C and Isotope MDO4-2861 (ka) (LRO4 age)	Refined age model (ka) (Ziegler et al., 2010a)	Age anomaly (ka)
GEl	370	17.2	17.4	0.2
GE3	800	38.5	39.5	1
GE6	1090	56	64.3	8.3
GE8	1330	88	85	3
GE9	1430	101	103.9	2.9
GEI0	1470	106	110	4
GEII	1620	126	130.5	4.5
GEI3	1900	156	158.2	2.2
GEI5	2340	196	191	5
GEI6	2600	219	225	6
GEI7	2800	241	250	9
GEI8	3110	271	266	5
GEI9	3350	293	296.9	3.9

record suggesting a strong influence of an open-ocean upwelling, and/or the effect of lateral advection via eddies and filaments associated with the coastal Oman upwelling (Fig. 1). Previous studies demonstrated that *G. glutinata* is more abundant in the open-ocean upwelling area and *G. bulloides* in the coastal upwelling area (Anderson and Prell, 1993; Ishikawa and Oda, 2007; Ivanova et al., 2003). *G.bulloides* is more abundant (mean values of 23%) than *G.glutinata* (mean values of 9%) in the core, suggesting a strong influence of the coastal upwelling area. The strong influence of the summer monsoon upwelling conditions on the distribution of *G. bulloides* is also confirmed by the study of Schulz et al. (2002). They found that *G. bulloides* is of minor importance in sediment trap off Pakistan, in an area strongly influenced by NE monsoon.

As the ecology of individual species is often hardly distinguishable from the community dynamics, we grouped ecologically related species to discuss our results. Following previous works (Conan and Brummer, 2000; Ishikawa and Oda, 2007; Ivanova et al., 1999; Schiebel et al., 2001) we define a planktonic foraminifera (PF) SW monsoon upwelling assemblage composed of *G. bulloides*, *N. pachyderma* (*sinistral* coiling), *G. glutinata*, *N. dutertrei*, *G. scitula*, *P. obliquiloculata*, *T. parkerae*, *G. hexagona*, *G. menardii* and *G. theyeri*. All these species represent SW monsoon conditions in the coastal upwelling area (Conan and Brummer, 2000; Peeters and Brummer, 2002) and underline the summer season (*G. bulloides*, *N. dutertrei*) or the autumn season (*G. glutinata*) in the Pakistan area (Schulz et al., 2002) (Fig. 3).

In contrast, *G. falconensis* dominates in flux and relative abundance in the Pakistan area (Schulz et al., 2002), and is indicative of winter mixing, when NE monsoonal winds cool the highly saline surface waters and break up stratification. In the coastal Oman upwelling, this species represent non upwelling condition (Conan and Brummer, 2000; Peeters and Brummer, 2002). This species is also present in our record and account for less than 4%, with an opposite pattern compared to the PF SW monsoon assemblage (Fig. 3). This confirms that fauna assemblages in our core site are mainly affected by SW monsoon over the last 310 ka. We build a planktonic foraminifera (PF) NE monsoon assemblage as the sum of *G. falconensis*, *G. aequilateralis*, *G. ruber*, *O. universa*, *G. sacculifer*, *G. trilobus*, *G. tenella*, *G. calida* and *G. uvula* (Fig. 3). All these species are associated to non upwelling condition and NE monsoon development (Conan and Brummer, 2000; Peeters and Brummer, 2002; Schulz et al., 2002). Fig. 3 shows an opposite behavior between PF SW monsoon assemblage and PF NE monsoon assemblage.

4.3. The grain size proxy

Grain size results are shown in Fig. 4. We used the D90 grain size parameter which corresponds to grain size at which 90% of sediments are finer. The curve indicates important variations over the last 310 ka. To determine which granulometric range is responsible for these variations, we have focused on the granulometric curves during key periods of the record (numbered 1 to 6 on Fig. 4). We observe two important modes on granulometric curves: a clay mode (corresponding to grain-size finer than 10 μm) and a silty mode (corresponding to 10–63 μm). Periods marked by a lower D90 grain size (periods 1, 3 and 5) correspond to high clay content and lower silt content. Inversely, a period marked by a higher D90 grain size (2, 4 and 6) is associated with lower clay content and a higher silty content. To evaluate if these changes are mainly related to lithogenic variability through times, we have applied the same approach based on carbonate free samples on the same intervals 3 and 4 (3′ and 4′ on Fig. 4). The results exhibit the same pattern, and thus demonstrate that lithogenic changes control the grain size evolution through times. In addition, carbonate content in the core is low and presents weak variation in amplitudes (between 15 and 30%) suggesting a dominant lithogenic component of sedimentation at our core site.

Because the grain size variations in the core are related to the balance between silty and mud content, we calculated the D50 of the

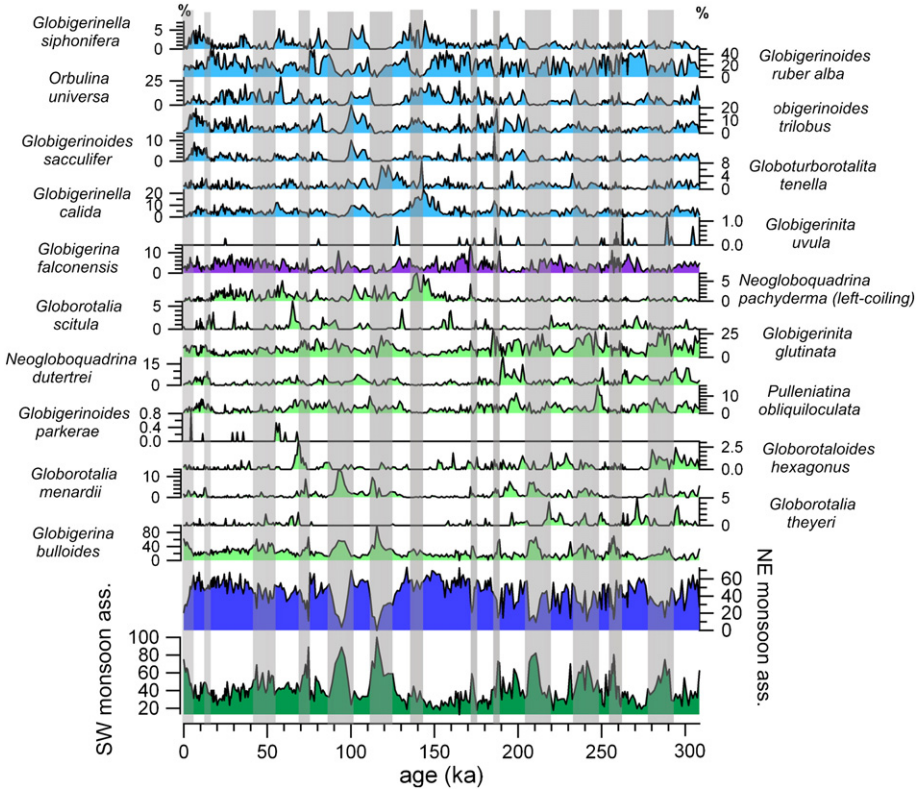

Fig. 3. SW and NE monsoon planktonic foraminifera assemblages (purple for the NE monsoon species *G. falconensis*, blue and purple for the NE monsoon assemblages, green for the SW monsoon assemblages). Frames indicate important increase/decrease events of SW/NE monsoon over the last 310 ka.

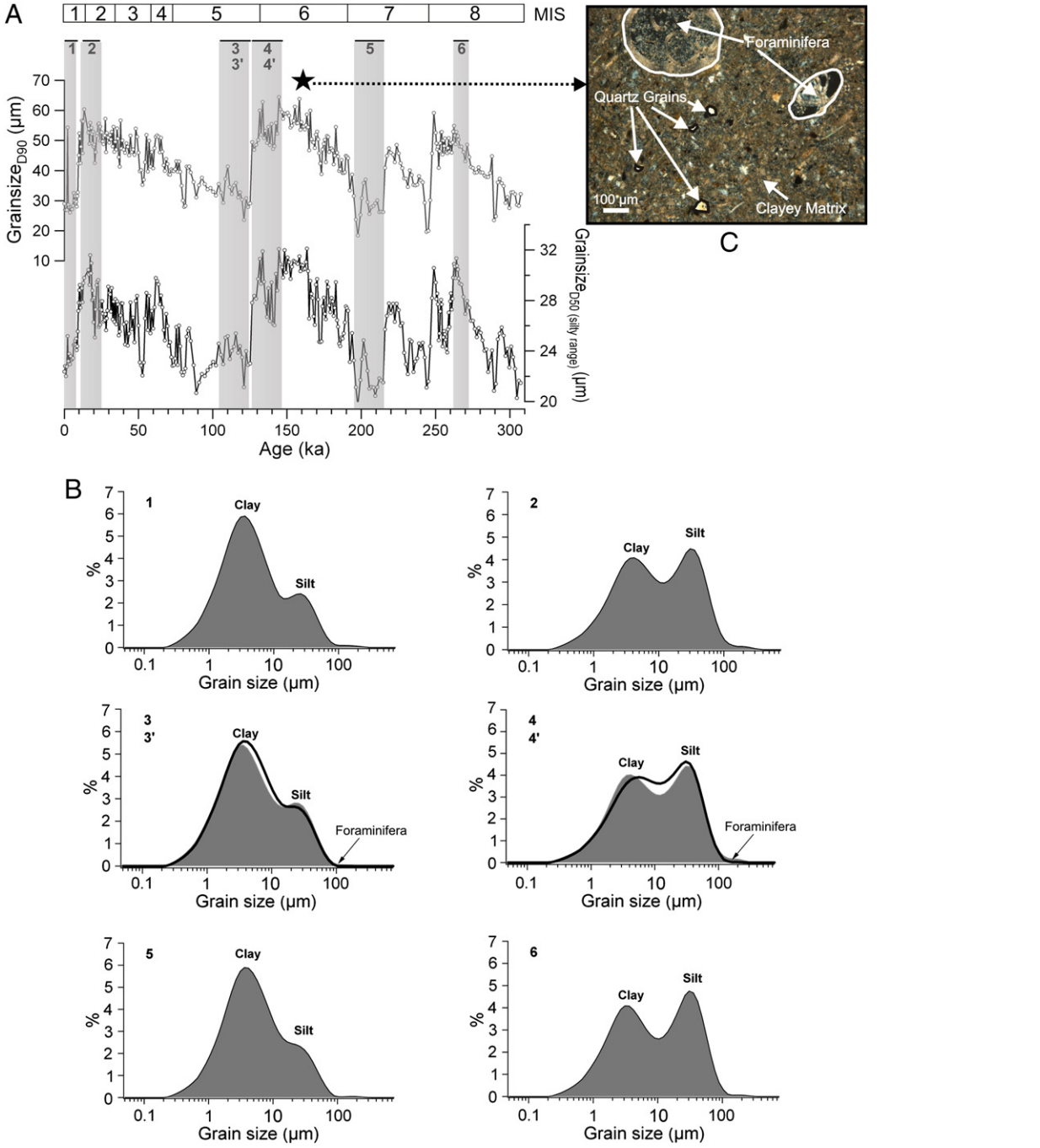

Fig. 4. Grain size results for core MD04-2861. A) D90 grain size parameter (which corresponds to grain size at which 90% of samples are finer) and D50 grain size of the silty range. B) Granulometric curve during key periods of the record (different numbers: the granulometric curves represent average samples for the periods considered: gray frames on A). We observe two dominant modes on the granulometric curves: a clay mode and a silty mode. Granulometric curves 3′ and 4′ (plain black lines) indicate the results on carbonate free samples. C) Location (black star in A) and observation in the core of a thin section in analyzed polarized light. The presence of foraminifera is indicated. Examples of poorly organized quartz grains in the clayey matrix are visible.

silty fraction (~9–66 µm) (Fig. 4). The results show an excellent agreement with the D90 grain size, thus confirming the role of the increase/decrease of the silty fraction on the global granulometric variations observed in core MD04-2861.

Observation of a thin section under the microscope in analyzed polarized light allowed us to do a high-resolution analysis of the texture and structure of the deposit (Fig. 4C). It confirmed the importance of the silty and clay fractions and the presence of isolated foraminifera shells, from which the mode is also encountered on granulometric curves (Fig. 4B). In the thin section, we observed silty grains and a few fine sand grains. These grains essentially consist of poorly organized quartz grains in a clayey matrix (Fig. 4C). This suggests that silt to sand grains are not resulting from the deposition of deep-sea current (turbidity current or contouritic current). We infer that these grains have been likely transported by distal fluvial plumes and/or winds and finally decanted in the water column.

Unlike lithogenic grain size proxies previously employed at pelagic sites and interpreted in the context of atmospheric transport (Clemens and Prell, 1991; Clemens et al., 2008; Pourmand et al., 2004), lithogenic grain size at this continental margin site is interpreted in the context of fluvial and aeolian processes. Indeed, grain-size variability of lithogenic marine sediments is influenced by several parameters including the

distance of sediment transport and its capacity (i.e. wind strength, hypopycnal or hyperpycnal plumes) and the initial composition of sediments in the source area.

Climate is often described as the first-order control on the sand-to-mud ratio in the watershed and at river mouths (Perlmutter and Mattews, 1989), by controlling the sediment yield/discharge ratio (Blum and Törnqvist, 2000). In the Makran area, monsoon-induced periods of continental aridity and humidity had a major impact on fluvial dynamics (Jain and Tandon, 2003), that in turn directly influenced the timing and nature of sediment delivery to the sea, as highlighted by the deep-water turbidite system growth during the Late Quaternary (Bourget et al., 2010). Continental aridity, during weak SW monsoon together with important NE monsoon, leaded to increasing sediment yield and production of coarse-grained sediments (due to the lack of vegetation) in the Makran rivers settings (Bourget et al., 2010; Jain and Tandon, 2003). Aridity could also enhance the transport of coarse particles at sea by more active aeolian activity. Intensified dust contributions by northwesterly winds from the Persian Gulf area during dry conditions have been demonstrated (Sirocko et al., 1991) as well as coarser grained sediments deposition during stadials on the Pakistan margin linked to intensified winter monsoonal winds (Pourmand et al., 2004; Reichart et al., 2004). Inversely, wetter periods (stronger SW monsoon) were associated to increase in vegetation cover, decreasing production of coarse-grained sediments, and enhanced fluvial discharge of finer-grained particles (Jain and Tandon, 2003). These humid periods were associated with more frequent mud-rich turbidity currents in the Arabian Sea (Bourget et al., 2010).

Overall, during the humid periods of the SW monsoon, climatically-driven conditions of sediment production and transport allow the transfer of finer-grained sediments to our coring site (whether the transport agent is aeolian or plume-advection related). Inversely during the NE monsoon intensification (arid periods), coarser sediments are preferentially transferred.

High-amplitude sea level changes through the Quaternary are known to have a great influence on the amount and nature of sediment transferred to the marine environment. Classically, low-stands of sea-level enhance an important transport of bulk sediments to the sea, through the fluvial systems directly feeding the coastlines (Posamentier and Vail, 1989). Inversely sea-level highstands are often associated with drowning of the continental shelf that form an area of sediment trapping and sorting. Highstands thus often result in sediment partitioning and enhance transfer of finer-grained material towards the sea (Posamentier and Vail, 1989).

This effect of sea level changes on the grain size record is probably important at the 100 ka cycle which corresponds to the more important changes in sea level (Glacial–interglacial changes with a difference of ~120 m; Bintanja et al., 2005) (Fig. 4A). Indeed, grain size signals seem to be influenced by glacial–interglacial changes (Fig. 4A). However, here we will focus on the higher-resolution changes occurring at the obliquity and precession cycle (41 and 23 ka cycle). These changes in grain size, together with the record from the bromine and foraminifera assemblage proxy, will be detailed in the following section.

4.4. Arabian Sea records and monsoon forcing/response relationship

4.4.1. Does the multi-proxy record from core MD04-2861 mirror an Indian monsoon dynamics?

The bromine signal obtained on core MD04-2861 and the composite Bromine signal obtained by Ziegler et al. (2010a) on the Murray ridge show consistency (Fig. 5). Interestingly, the SW monsoon foraminifera assemblage variations throughout time also mirrors bromine fluctuations (increase of the PF SW monsoon assemblage during increase of bromine; Fig. 5) although our coring site, located in a northern position in the Arabian Sea was supposed to

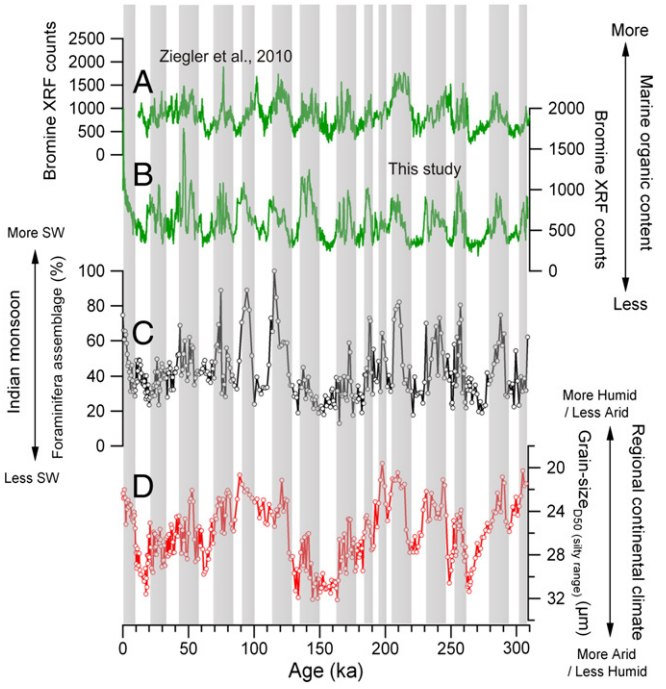

Fig. 5. Comparison of independent SW monsoon proxies. A) Bromine data after Ziegler et al. (2010a). B) Bromine data in core MD04-2861 (this study). C) Planktonic foraminifera SW monsoon assemblage variation in core MD04-2861. D) D50 (silty range) grain size variation in core MD04-2861. Gray bands underline periods of high Bromine (MOContent) in core MD04-2861. They coincide with increases in PF SW monsoon assemblage together with decrease in grain size interpreted as period of SW monsoonal intensification.

be also influenced by the NE monsoon (Fig. 1). This suggests that, as southerly sites (Clemens and Prell, 2003; Clemens et al., 2008), our record is mainly controlled by the SW monsoon dynamics. SW upwelling reinforcement boosting surface productivity could thus also impact the marine organic content (MOContent) signal in the northern Arabian Sea sedimentological archives. Variability in the grain size is also in good agreement with the bromine and the PF SW monsoon assemblage (Fig. 5) with grain size minima observed in conjunction with increasing bromine values and a larger representativity of the PF SW monsoon assemblage (gray frames on Fig. 5).

To determine if sea level variability in the precession and obliquity orbital bands can control the observed grain size variations, we have determined the timing of grain size changes and sea level changes (Fig. 6A). For the precession band, grain size minimum lag precession minimum by 8.3 ± 0.5 ka, clearly not in phase with the lag between high sea level (Waelbroeck et al., 2002) and the minima of precession which is of 4.9 ± 0.4 ka (Fig. 6A).

Our results show that each SW monsoon intensification events during the last 310 ka have been associated to finer-grained sedimentation in core MD04-2861 (increasing clay content and decreasing silt content; Fig. 5) which is controlled by a more humid regional continental climate at those times. The phase relationship of fine grain sedimentation is consistent with previous estimation of the SW monsoon timing in the precession band (Clemens et al., 2010) (Fig. 6A). We have also estimated the phasing for the other proxies (foraminifera assemblage and Bromine data). We found a lag of 8.9 ± 0.7 ka between maximum SW monsoon upwelling assemblage and the minimum of precession and 9.7 ± 0.4 ka between maximum of bromine signal and the minimum of precession (Fig. 6A). The grain size proxy cannot be influenced by nutrient changes associated with AMOC, yet has the same phase as the productivity proxies, proving that the productivity proxies (bromine) have the same timing as strengthened summer monsoons (Fig. 6A). These phase relationships indicates that decreased ice volume and increased latent heat export from the

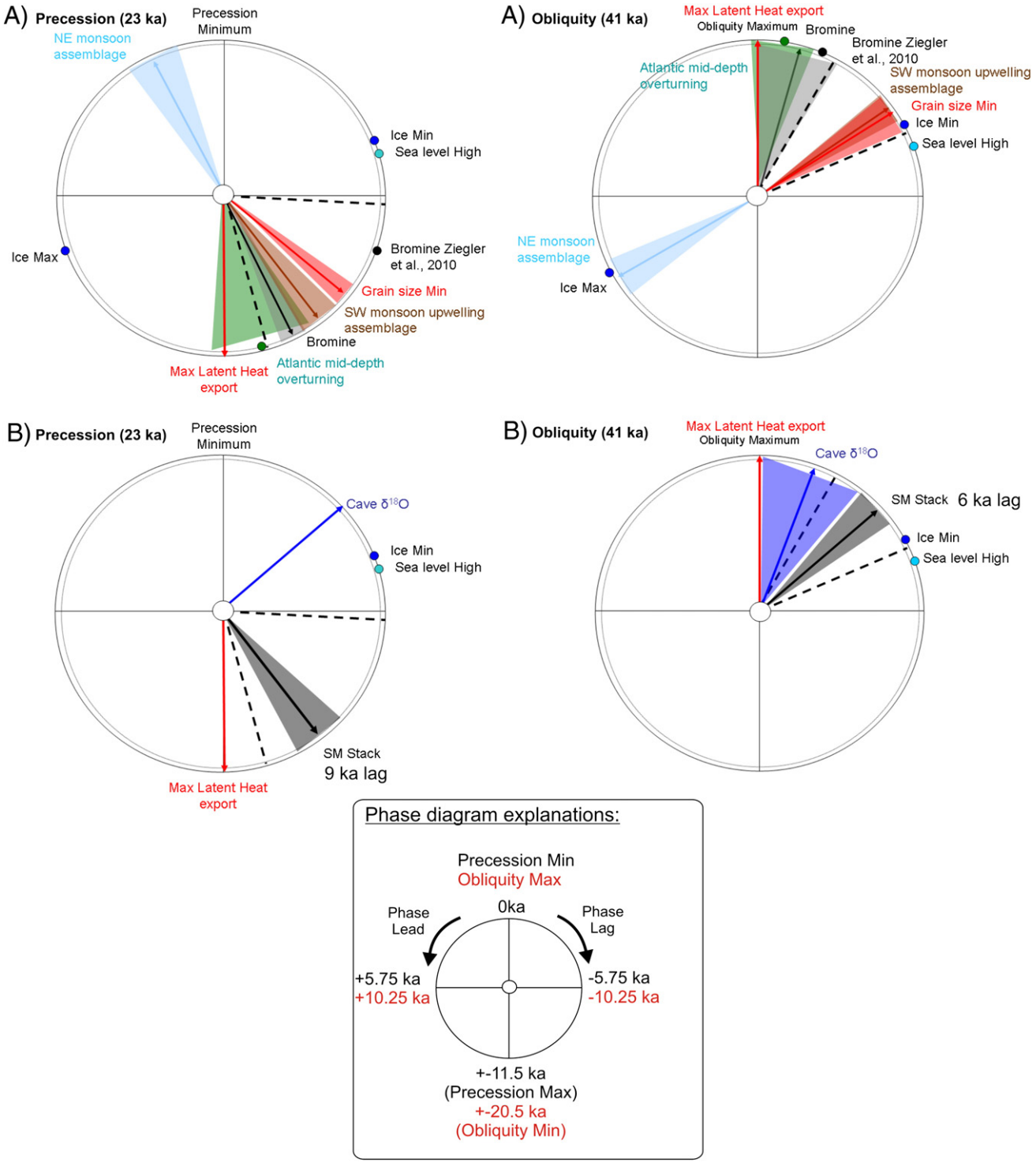

Fig. 6. Cross-spectral coherence and phase wheel summaries. The diagrams shows the Arabian sea records response to insolation forcing at the orbital obliquity (41 ka) and precession (23 ka) periods for A) each independent Arabian Sea proxies and B) the SM stack and Asian speleothems. The precession index is defined as $\Delta e \sin w$ where w is the longitude of perihelion measured from the moving vernal point and e is the eccentricity of Earth's orbit about the sun (Berger, 1978; Laskar et al., 2004). Obliquity is the tilt of Earth's axis with respect to the plane of the ecliptic. Zero phase is set at precession minima and obliquity maxima. Negative phases are measured in the clockwise direction representing temporal lags (see phase diagram explanations).Vector length represents coherence (dotted circle marks 95%). Shaded areas represent 95% confidence interval of the phase estimate. Phase relationship with Atlantic mid-depth overturning (Lisiecki et al., 2008), ice volume (Lisiecki and Raymo, 2005), sea level (Waelbroeck et al., 2002), Bromine (Ziegler et al., 2010a) and the max latent heat export from the southern Indian Ocean (Clemens et al., 2008) are indicated. Intervals delimited by black dashed lines indicate the timing of summer Indo-Asian monsoon in the precession band (Clemens et al., 2010) and in the Obliquity band (Clemens et al., 2008).

southern Indian Ocean set the timing of strong summer monsoons within the precession cycle and that direct sensible heating initiate monsoonal circulation (Clemens et al., 2008) (Fig. 6). Interestingly, Indian winter monsoon (WM), documented by the NE foraminifera assemblage (Fig. 3), occurs between ice maxima and northern hemisphere sensible heat minima, indicating that both act to strengthen WM circulation (Fig. 6A). The SW and NE monsoon are in antiphase in the precession band and suggest that the two systems are dynamically linked (Fig. 6A). Similar results have been found for the Asian monsoon (Clemens et al., 2008) and could indicate a link between Indian and

Asian WM. This also demonstrates that productivity proxy (bromine) is not affected by WM but clearly controlled by strengthened summer monsoons.

In the Obliquity band, minimum grain size (increase of clay content in the core) lag by 7.2 ± 1.3 ka the maximum of obliquity, close to what is observed for sea level changes (lag of 7.9 ± 1.4 ka), but however more consistent with previous estimate timing of the SW monsoon (Fig. 6A) (Clemens et al., 2008). According to our previous hypothesis suggesting that sea level is not the main driver of grain size changes observed in the precession band, we can also hypothesis that SW monsoon is the main driver of the observed timing in the obliquity band. The lag of 6.9 ± 1 ka between the maximum of SW monsoon upwelling assemblage and maximum obliquity, and the lag of 2.4 ± 2.4 ka between the maximum of bromine and maximum obliquity confirm our hypothesis (Fig. 6A). As for the precession band, the strong SW monsoon in the northern Arabian Sea falls between ice minima and sensible/latent heat maxima indicating that all three forcing could act together to strengthen summer monsoon circulation (Clemens et al., 2008). The WM proxy (NE foraminifera assemblage) occurs between ice maxima and sensible heat minima, when considering uncertainties and the two different age models (Fig. 6A and supplementary Table 2), indicating that both act to strengthen WM circulation. Again, similar results have been found for the Asian monsoon (Clemens et al., 2008).

4.4.2. An Indian summer monsoon stack from the northern Arabian Sea

Bromine, PF SW monsoon upwelling assemblage and grain size in core MD04-2861 are mainly controlled by SW monsoon dynamics. Although all monsoonal proxies likely respond to monsoon variability, additional processes, sometimes unrelated to monsoon circulation (e.g. preservation, dissolution, diagenesis), may also influence the chemical, physical and biological compositions of sedimentary archives (Clemens and Prell, 2003). To limit such biases, we decided to stack the independent records of monsoon intensity using principal components analysis (PCA) in order to derive a more robust, combined record of monsoon variability and allow comparison with previous monsoon stack in the region (Clemens and Prell, 2003).

Contrary to the stack of Clemens and Prell (2003) and in response to Ziegler et al. (2010a) hypothesis, our stack is not a productivity stack. Bromine is a productivity proxy, the faunal assemblage is influenced by productivity changes but is also strongly influenced by sea-surface abiotic parameters (temperature, salinity, stratification) (Conan and Brummer, 2000; Murray, 1897; Peeters and Brummer, 2002), and grain size signal is independent of productivity and directly related to the regional continental climate.

PCA, performed with the "R" software (http://www.r-project.org/), indicates that the first component (PC1: i.e. the summer monsoon (SM) stack) of all our record (grain size, bromine and foraminifera assemblage) explains 69% of common variance compared to the only 33% of variance contained in the monsoon stack of Clemens and Prell (2003), clearly showing that all our proxies are mainly controlled by the same common forcing, the SW monsoon dynamics. Note that each individual proxies were resampled with a common resolution of 1 ka for the building of the Arabian SM stack (the resolution for each individual proxies was better than 1 ka) and that this resolution is higher than the one used for the SM stack of Clemens and Prell (2003) (2 ka). Maximum of the SM stack lag maximum northern hemisphere (NH) summer insolation by 9 ± 1 ka in the precession band and by 6 ± 1.3 ka in the obliquity band (Fig. 6B supplementary Table 2 and Fig. 3). The observed timing is consistent with recent studies based on a large number of Indian and East-Asian proxies from marine, lakes and terrestrial archives, except Asian speleothems (Figs. 7 and 8 and supplementary Table 2)(Clemens et al., 2008, 2010; Ziegler et al., 2010a) but is not reproduced by modeling experiments (Kutzbach et al., 2008; Ziegler et al., 2010a). The non-consistency with numerical simulation results could be related to some model limitations. There is no model run yet

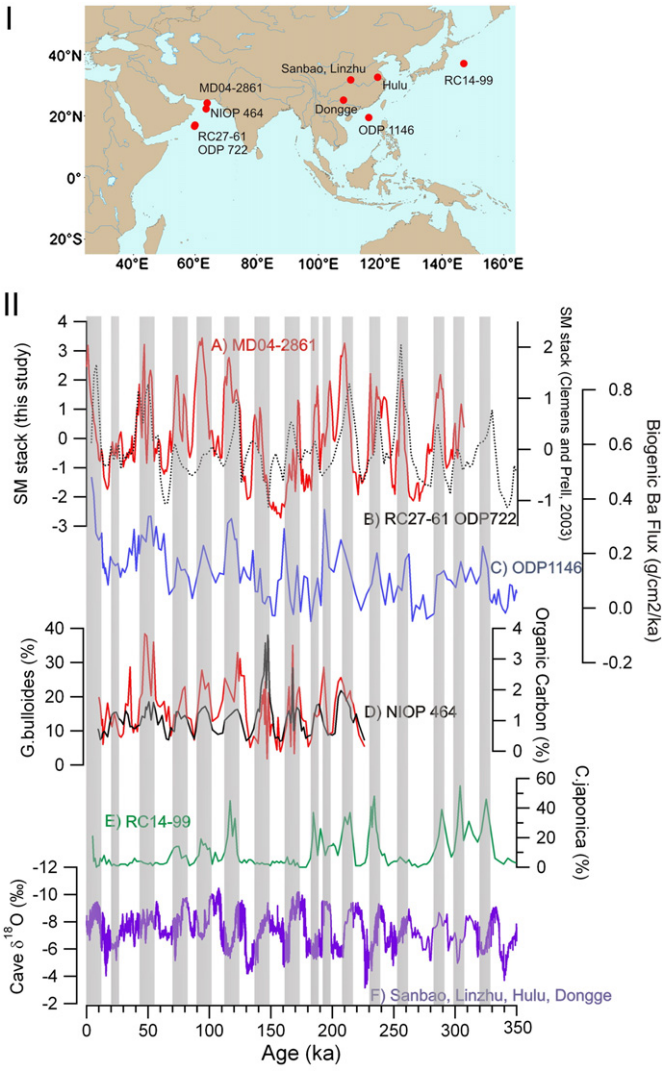

Fig. 7. Comparison of our SM stack with other Indo-Asian monsoon proxies. I) location of the different Indo-Asian monsoon records. II) A) Indian SM stack for this study (MD04-2861). B) Indian SM stack (Clemens and Prell, 2003). C) Productivity (runoff) at site ODP 1146 (Clemens et al., 2008). D) Productivity (upwelling) at site NIOP 464 (Reichart et al., 1998). E) Precipitation at the Philipine Sea (Morley and Heusser, 1997). F) Precipitation with Asian speleothems (Cheng et al., 2009; Dykoski et al., 2005; Wang et al., 2001; 2008). A graphical correlation suggests that variations detected in Indo-Asian monsoon proxies are in good concordance with our SM stack (frames) except for Asian speleothems. Records are plotted on their original age scales.

available that is capable of assessing phase of the late Pleistocene summer monsoon systems given the complex lower boundary conditions (ice volume, sea level, and greenhouse gasses) involved. The Kutzbach et al. (2008) model lays on insolation conditions only, while the CLIMBER II model in Ziegler et al. (2010a), which is a great start, has a very low resolution and exhibits an unreal linearity to insolation.

4.4.3. Testing the effect of Atlantic overturning changes on the Arabian Sea productivity records

Our northern Arabian Sea proxies are strongly influenced by Indian monsoon forcing and in agreement with the timing found by Clemens and Prell (2003), Clemens et al. (2008, 2010) and Reichart et al. (1998), supporting the idea that the Arabian Sea records are mainly controlled by the Indian monsoon processes. However a recent study has proposed that the summer (SW) monsoon is unlikely the main driver of changes in Arabian Sea biological productivity and OMZ intensity at the precession frequency band (Ziegler et al., 2010a). By extrapolating the Schmittner et al. (2007) work from millennial scales

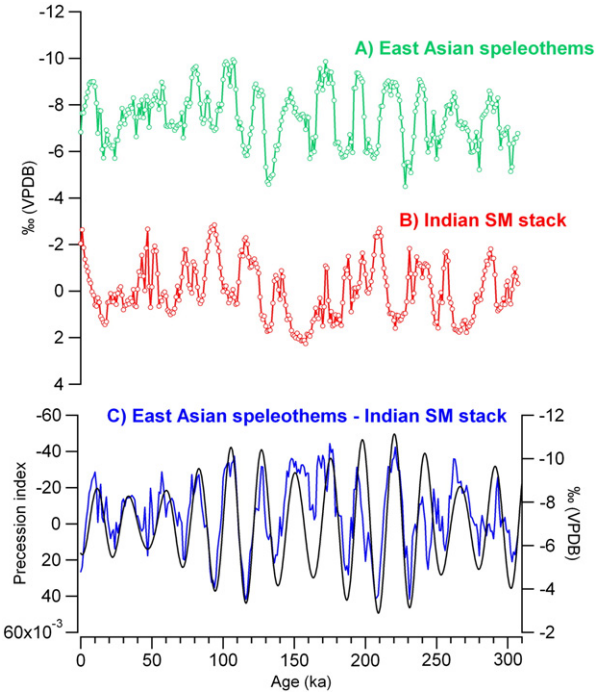

Fig. 8. Comparison of the Indian SM stack and Asian cave speleothems. A) Asian cave speleothems (Cheng et al., 2009; Dykoski et al., 2005; Wang et al., 2001; 2008) resample with a step of 1 ka. B) Indian SM stack with a resolution of 1 ka. C) Residual signal after the Indian SM stack subtraction from the Asian cave speleothems. The residual is highly coherent and in phase with precession minima suggesting an impact of winter temperature changes on cave $\delta^{18}O$ (Clemens et al., 2010).

to orbital scales, this new hypothesis proposed that changes in the intensity of the AMOC might have played the prominent role. The phase relationship of Atlantic overturning changes is visible in Fig. 6A through mid-depth benthic $\delta^{13}C$ gradient (a proxy indicator of ocean nutrient content) throughout the Atlantic (Lisiecki et al., 2008). Although the Schmittner et al. (2007) model does not produce an OMZ in the Arabian Sea and that the timing and the effect on Atlantic overturning circulation changes is complex and still under debate (Liu et al., 2005; Marchitto and Broecker, 2006; McManus et al., 2004; Negre et al., 2010; Yu et al., 1996), following Ziegler et al. (2010a), we address his potential role in controlling productivity signal in the Arabian Sea at orbital scale changes.

We note that the bromine signal of Ziegler et al. (2010a) and our bromine signal in core MD04-2861 exhibit a close timing in the precession and obliquity band, although one was retrieved within the OMZ water-depth interval and the other below the present OMZ (Fig. 6A and supplementary Fig. 1). We can therefore conclude that dynamics of the OMZ in the past, and its potential impact on the preservation of the MOContent in the sediment is not the main driver of both signals observed, as previously suspected (Reichart et al., 1998). The ~2.5 ka differences observed in the precession band between both bromine records (Fig. 9) could results from uncertainties during age model constructions or could reflect differences between XRF core scanner methods.

Interestingly, the phase relationship for our Bromine record presents a pattern which, compared to the PF SW monsoon assemblage and grain size data, seems to be the closest to the timing of the Atlantic mid-depth overturning (Lisiecki et al., 2008) at both precession and obliquity cycle (Fig. 6A). This could suggest an effect of overturning changes on the Arabian Sea productivity record as hypothesized by Ziegler et al. (2010a). Nonetheless, the good coherency between the bromine record and our productivity-partly-independent/-independent SW monsoon proxies (PF assemblage and grain-size), supports that the SW monsoon remains the main driver of the timing observed in Arabian Sea productivity records. Caley et al. (in press) have also demonstrated that the exceptional productivity signal recorded in the Arabian sea during the atypical MIS 13 period (Ziegler et al., 2010c) could be explained by the combination of strong monsoon winds together with an additional, but secondary, effect of an increasing overturning circulation. Nonetheless, a secondary effect of overturning changes on the Arabian Sea productivity records is valuable only if intermediate water flows are not in antiphase with changes in the North Atlantic Ocean (Jung et al., 2009; Pahnke and Zahn, 2005). Indeed, a recent study demonstrated that increases in intermediate water flow in the Arabian Sea (Jung et al., 2009) and also in the Indo-southwestern Pacific (Pahnke and Zahn, 2005) occurred in anti-phase with changes in the North Atlantic Ocean during Henrich events (HE). This is in contradiction to a reduced export of nutrient-rich waters from the Atlantic into the Indian and Pacific euphotic zone which could lead to a decline of the export production in the Arabian Sea during HE. Because productivity decreased in the Arabian Sea during HE (Altabet et al., 2002), this suggests that changes in the intermediate ventilation is not the main driver of productivity changes, but are rather forced by the intensity of summer monsoon upwelling (Altabet et al., 2002; Honjo et al., 1999).

4.4.4. Comparison between East Asian speleothem record and our Indian SM stack

The idea that Indian and Asian monsoon are linked is derived from modern summer precipitations which are coherent and in phase with moisture transport from the southern Indian Ocean and out of phase with the moisture transport from the Pacific Ocean (Liu and Tang, 2004). Therefore, both Indian monsoon variability (recorded by our summer monsoon (SM) stack) and Asian monsoon variability (recorded by the Asian speleothems) might exhibit the same pattern. This is however not supported by our results (Figs. 7 and 8), neither by the reanalyses of Asian speleothems conducted in Clemens et al. (2010). To explain these differences, we can call for different seasonal controls on records. To extract the summer monsoon component of the Asian speleothems, Clemens et al. (2010) have built a SM orbital model. Here, our Indian SM stack is based on orbitally-independent age constrain derived from the correlation of GEs in our record to those of Ziegler et al. (2010a). The speleothem records are also based on U/Th-derived ages. That strengthens our confidence in using both age scales for the same calculation.

We normalized our SM stack and we transferred the scale in ‰ units by multiplying by the total variance in cave $\delta^{18}O$ (Fig. 8B). Then, we subtracted the SM stack (Fig. 8B) from the Asian cave $\delta^{18}O$ (Fig. 8A) and find a residual highly coherent and in phase with precession minima (Fig. 8C and supplementary Fig. 4). During minima of precession, northern hemisphere winters were extremely colder (Berger, 1978). Clemens et al. (2010) proposed that this residual signal reflect the influence of the winter monsoon, consistent with modern seasonality in precipitation amount and isotopic composition (they call on winter atmospheric precipitation temperature changes to drive the signal). Therefore, our results support the idea that Asian speleothems cannot be interpreted as reflecting only the timing of strong summer monsoon (Clemens et al., 2010).

5. Conclusion

Multiproxies analysis (bromine, foraminifera assemblages and grain size) of a marine sediment record located off the Makran margin revealed that productivity signals (Bromine) in the northern Arabian Sea are mainly controlled by SW monsoon dynamics rather than by NE monsoon dynamics or changes in the intensity of the Atlantic meridional overturning circulation (AMOC) (Ziegler et al., 2010a). The use of three independent SW monsoon proxies allowed us to build a robust Indian summer monsoon stack on an age model not relying upon orbital assumptions over the last 310 ka with a resolution of 1 ka. For the phase relationship of our SM stack, a 9 ± 1 ka lag is found

between external forcing (maximum NH summer insolation) and strong Indian SW monsoon in the precession band and a lag of 6 ± 1.3 ka in the obliquity band between forcing and response. These results are consistent with numerous Indo-Asian summer monsoon records (Clemens and Prell, 2003; Clemens et al., 2008, 2010; Ziegler et al., 2010a) and has large implications:

- this indicate that internal climate forcing such as decreased ice volume and increased latent heat export from the southern Indian Ocean (Clemens et al., 2008) set the timing of strong Indo-Asian summer monsoons within both the precession and obliquity cycle and that direct sensible heating (the external forcing) initiate monsoonal circulation. At the moment, this observation is not reproduced by modeling experiments (Kutzbach et al., 2008; Ziegler et al., 2010a).
- this suggests that East Asian speleothems cannot reflect the timing of strong summer monsoon alone and are probably impacted by winter temperature changes as already suggested by Clemens et al. (2010).
- this also suggests that the forcing/response relationship of the Indo-Asian monsoon in the precession cycle is different to what occurs for African monsoons and suggest that the concept of a "global monsoon" at orbital scale changes is a misnomer (Caley et al., submitted for publication).

Acknowledgements

We are indebted to all scientists, technicians and crew members of the R/V Marion-Dufresne for technical assistance during the CHAMAK cruise. The authors are also grateful to E. Moreno at the MNHN, and J. St. Paul, G. Chabaud, B. Martin, M.H Castéra, I. Billy (University of Bordeaux) for their logistical and technical assistance. The authors would like to acknowledge S.C. Clemens and the editor P.B. deMenocal for their suggestions which help to significantly improve the final manuscript. The "ARTEMIS" radiocarbon dating project and CNRS INSU LEFE-EVE program "MOMIES" are acknowledged. This paper is contribution 1831 of UMR 5805 EPOC, University Bordeaux 1.

Appendix A. Supplementary data

Supplementary data to this article can be found online at doi:10.1016/j.epsl.2011.06.019.

References

Altabet, M.A., Higginson, M.J., Murray, R.W., 2002. The effect of millennial-scale changes in the Arabian Sea denitrification on atmospheric CO2. Nature 415, 159–162.
Anderson, D.M., Prell, W.L., 1993. A 300 kyr record of upwelling off Oman during the late Quaternary: evidence of the Asian southwest monsoon. Paleoceanography 8, 193–208.
Bard, E., 1998. Geochemical and geophysical implications of the radiocarbon calibration. Geochim. Cosmochim. Acta 62, 2025–2038.
Berger, A., 1978. Long-term variations of daily insolation and Quaternary climate change. J. Atmos. Sci. 35, 2362–2367.
Bintanja, R., Van de Wal, R., Oerlemans, J., 2005. Modelled atmospheric temperatures and global sea levels over the past million years. Nature 437, 125–128.
Blum, M.D., Törnqvist, T.E., 2000. Fluvial responses to climate and sea-level change: a review and look forward. Sedimentology 47, 2–48.
Bourget, J., Zaragosi, S., Ellouz-Zimmermann, S., Ducassou, E., Prins, M.A., Garland, T., Lanfumey, V., Schneider, J.-L., Rouillard, P., Giraudeau, J., 2010. Highstand vs. lowstand turbidite system growth in the Makran active margin: imprints of high-frequency external controls on sediment delivery mechanisms to deep water systems. Mar. Geol. 274, 187–208.
Bourget, J., Zaragosi, S., Ellouz-Zimermann, N., Mouchot, N., Garlan, T., Schneider, J.-L., Lanfumey, V., Lallemant, S., 2011. Turbidite system architecture and sedimentary processes along topographically complex slopes: the Makran convergent margin. Sedimentology 58, 376–406. doi:10.1111/j.1365-3091.2010.01168.x.
Caley, T., Malaizé, B., Bassinot, F., Clemens, S.C., Caillon, N., Linda, R., Charlier, K., Rebaubier, H., in press. The monsoon imprint during the 'atypical' MIS 13 as seen through North and Equatorial Indian Ocean records. Quaternary Research.
Cheng, H., Edwards, R.L., Broecker, W.S., Denton, G.H., Kong, X., Wang, Y., Zhang, R., Wang, X., 2009. Ice Age terminations. Science 326, 248–252.
Clemens, S.C., Prell, W.L., 1991. One million year record of summer monsoon winds and continental aridity from the owen ridge (site 722), northwest Arabian sea. Proceedings of the ocean drilling program, Scientific results, Vol. 117.
Clemens, S.C., Prell, W.L., 2003. A 350,000 year summer-monsoon multiproxie stack from the Owen ridge, Northern Arabian Sea. Mar. Geol. 201, 35–51.
Clemens, S.C., Murray, D.W., Prell, W.L., 1996. Nonstationary phase of the plio-pleistocene Asian Monsoon. Science 274, 943–948.
Clemens, S., Prell, W.L., Sun, Y., Liu, Z., Chen, G., 2008. Southern Hemisphere forcing of Pliocene $\delta^{18}O$ and the evolution of Indo-Asian monsoons. Paleoceanography 23, PA4210. doi:10.1029/2008PA001638.
Clemens, S.C., Prell, W.L., Sun, Y., 2010. Orbital-scale timing and mechanisms driving Late Pleistocene Indo-Asian summer monsoons: reinterpreting cave speleothem $\delta^{18}O$. Paleoceanography 25, PA4207. doi:10.1029/2010PA001926.
Conan, S.M.-H., Brummer, G.-J.A., 2000. Fluxes of planktic foraminifera in response to monsoonal upwelling on the Somalia Basin margin. Deep-Sea Res. II 47, 2207–2227.
Dykoski, C.A., Edwards, R.L., Cheng, H., Yuan, D., Cai, Y., Zhang, M., Lin, Y., Qing, J., An, Z., Revenaugh, J., 2005. A high-resolution, absolute-dated Holocene and deglacial Asian monsoon record from Dongge Cave, China. Earth Planet. Sci. Lett. 233, 71–86.
Ellouz-Zimmermann, N., Deville, E., Müller, C., Lallemant, S., Subhani, A.B., Tabreez, A.R., 2007. Impact of sedimentation on convergent margin tectonics: example of the Makran Accretionary prism (Pakistan). In: Lacombe, O., Lavé, J., Roure, F., Verges, J. (Eds.), Thrust Belts and Foreland Basins.
Hemleben, C., Spindler, M., Erson, O.R., 1989. Modern planktonic foraminifera. Springer, Berlin. 363 pp.
Honjo, S., Dymond, J., Prell, W., Ittekkotd, V., 1999. Monsoon-controlled export fluxes to the interior of the Arabian Sea. Deep-Sea Res. II 46, 1859–1902.
Imbrie, J., Hays, J.D., Martinson, D.G., McIntyre, A., Mix, A.C., Morley, J.J., Pisias, N.G., Prell, W.L., Shackelton, N.J., 1984. The orbital theory of Pleistocene climate: support from a revised chronology of the marine $\delta^{18}O$ record. In: Berger, A.L., et al. (Ed.), Milankovitch and Climate: Understanding the Response to Astronomical Forcing. D. Reidel, Hingham, Mass, pp. 269–305.
Ishikawa, S., Oda, M., 2007. Reconstruction of Indian monsoon variability over the past 230,000 years: planktic foraminiferal evidence from the NW Arabian Sea open-ocean upwelling area. Mar. Micropaleontol. 63, 143–154.
Ivanova, E.M., Conan, S.M.-H., Peeters, F.J.C., Troelstra, S.R., 1999. Living Neogloboquadrina pachyderma sin and its distribution in the sediments from Oman and Somalia upwelling areas. Mar. Micropaleontol. 36, 91–107.
Ivanova, E.M., Schiebel, R., Singh, A.D., Schmiedl, G., Niebler, H.-S., Hemleben, C., 2003. Primary production in the Arabian Sea during the last 135000 years. Palaeogeog. palaeoclim. palaeoecol. 197, 61–82.
Jaeschke, A., Ziegler, M., Hopmans, E.C., Reichart, G.J., Lourens, L.J., Schouten, S., Sinninghe Damsté, J.S., 2009. Molecular fossil evidence for anaerobic ammonium oxidation in the Arabian Sea over the last glacial cycle. Paleoceanography 24, PA2202. doi:10.1029/2008PA001712.
Jain, M., Tandon, S.K., 2003. Fluvial response to Late Quaternary climate changes, western India. Quat. Sci. Rev. 22, 2223–2235.
Jung, S.J.A., Kroon, D., Ganssen, G., Peeters, F., Ganeshrama, R., 2009. Enhanced Arabian Sea intermediate water flow during glacial North Atlantic cold phases. Earth Planet. Sci. Lett. 280, 220–228. doi:10.1016/j.epsl.2009.01.037.
Kennett, J.P., Srinivasan, M.S., 1983. Neogene Planktonic Foraminifera: A Phylogenetic Atlas Hutchinson Ross. Stroudsburg, PA.
Kukowski, N., Schillhornb, T., Huhna, K., von Radc, U.S.H., Fluehb, E.R., 2001. Morphotectonics and mechanics of the central Makran accretionary wedge off Pakistan. Mar. Geol. 173, 1–19.
Kutzbach, J.E., Liu, X., Liu, Z., Chen, G., 2008. Simulation of the evolutionary response of global summer monsoons to orbital forcing over the past 280,000 years. Clim. Dyn. 30, 567–579.
Laskar, J., Robutel, P., Joutel, F., Gastineau, M., Correia, A.M.C., Levrard, B., 2004. A long-term numerical solution for the insolation quantities of the Earth. A & A 428, 261–285.
Lisiecki, L.E., Raymo, M.E., 2005. A Pliocene–Pleistocene stack of 57 globally distributed benthic $\delta^{18}O$ records. Quat. Sci. Rev. 20.
Lisiecki, L.E., Raymo, M.E., Curry, W.B., 2008. Atlantic overturning responses to Late Pleistocene climate forcings. Nature 456. doi:10.1038/nature07425.
Liu, T., Tang, W., 2004. Oceanic influence on the precipitation in India and China as observed by REMM and QuikSCAT. Paper presented at The 2nd International Tropical Rainfall Measuring Mission Science Conference. Jpn. Aerosp. Explor. Agency, Tokyo.
Liu, Z., Shin, S., Webb, R.S., Lewis, W., Otto-Bliesner, B.L., 2005. Atmospheric CO2 forcing on glacial thermohaline circulation and climate. Geophys. Res. Lett. 32, L02706. doi:10.1029/2004GL021929.
Luckge, A., Doose-Rolinski, H., Khan, A.A., Schulz, H., von Rad, U., 2001. Monsoonal variability in the northeastern Arabian Sea during the past 5000-years: geochemical evidence from laminated sediments. Palaeogeog. palaeoclim. palaeoecol. 167 (3–4), 273–286.
Marchitto, T.M., Broecker, W.S., 2006. Deep water mass geometry in the glacial Atlantic ocean: a review of constraints from the paleonutrient proxy Cd/Ca. Geochem. Geophys. Geosyst. 7, Q12003. doi:10.1029/2006GC001323.
Martrat, B., Grimalt, J.O., Shackleton, N.J., de Abreu, L., Hutterli, M.A., Stocker, T.F., 2007. Four climate cycles of recurring deep and surface water destabilizations on the Iberian Margin. Science 317, 502–507. doi:10.1126/science.1139994.
McManus, J.F., Francois, R., Gherardi, J.-M., Keigwin, L.D., Brown-Leger, S., 2004. Collapse and rapid resumption of Atlantic meridional circulation linked to deglacial climate changes. Nature 428, 834–837.
Morley, J.J., Heusser, L.E., 1997. Role of orbital forcing in east Asian monsoon climates during the last 350 kyr: evidence from terrestrial and marine climate proxies from core RC14-99. Paleoceanography 12, 483–493.

Murray, J., 1897. On the distribution of the pelagic foraminifera at the surface and on the floor of the ocean. Nat. Sci. Ecol. 11, 17–27.
Negre, C., Zahn, R., Thomas, A.L., Masque, P., Henderson, G.M., Martinez-Mendez, G., Hall, I.R., Mas, J.L., 2010. Reversed flow of Atlantic deep water during the Last Glacial Maximum. Nature 468. doi:10.1038/nature09508.
Pahnke, K., Zahn, R., 2005. Southern hemisphere water mass conversion linked to North Atlantic climate variability. Science 307, 1741–1746.
Paillard, D., Labeyrie, L.D., Yiou, P., 1996. Macintosh program performs time-series analysis. Eas.Trans. 77–379.
Peeters, F., Brummer, G.-J.A., 2002. The seasonal and vertical distribution of living planktic foraminifera in the NW Arabian Sea. In: Clift, P.D., et al. (Ed.), The Tectonic and Climatic Evolution of the Arabian Sea Region, 195. Geological Society Special Publication, pp. 463–497.
Perlmutter, M.A., Mattews, M.D., 1989. Global cyclostratigraphy—a model. In: Cross, T.A. (Ed.), Quantitative Dynamic Stratigraphy. Prentice-Hall, Englewood Cliffs, pp. 233–260.
Posamentier, H.W., Vail, P.R., 1989. Eustatic controls on clastic deposition II—sequence and systems tract models. In: Wilgus, al (Eds.), Sea-Level Changes: An Integrated Approach. SEPM Special Publication, Tulsa, pp. 125–154.
Pourmand, A., Marcantonio, F., Schulz, H., 2004. Variations in productivity and eolian fluxes in the northeastern Arabian Sea during the past 110 ka. Earth Planet. Sci. Lett. 221, 39–54.
Prins, M.A., Postma, G., 2000. Effects of climate, sea level, and tectonics unraveled for last deglaciation turbidite records of the Arabian Sea. Geology 28, 375–378.
Reichart, G.J., Lourens, L.J., Zachariasse, W.J., 1998. Temporal variability in the northern Arabian Sea oxygen minimum zone (OMZ) during the last 225,000 years. Paleoceanography 13, 607–621.
Reichart, G.J., Brinkhuis, H., Huiskamp, F., Zachariasse, W.J., 2004. Hyperstratification following glacial overturning events in the northern Arabian Sea. Paleoceanography 19, PA2013. doi:10.1029/2003PA000900.
Richter, T., Van Der Gast, S.J., Kostner, B., Vaars, A., Gieles, R., Stigter, H., Haas, H., Weering, T., 2006. The Avaatech XRF Core Scanner: technical description and applications to NE Atlantic sediments, in New Techniques in Sediment Core Analysis. Geol. Soc. 267, 39–50.
Schiebel, R., Waniek, J., Borka, M., Hemlebena, C., 2001. Planktic foraminiferal production stimulated by chlorophyll redistribution and entrainment of nutrients. Deep-Sea Res. I 48, 721–740.
Schmiedl, G., Mackensen, A., 2006. Multi-species stable isotopes of benthic foraminifers reveal past changes of organic matter decomposition and deepwater oxygenation in the Arabian Sea. Paleoceanography 21, PA4213. doi:10.1029/2006PA001284.
Schmittner, A., Galbraith, E.D., Hostetler, S.W., Pedersen, T.F., Zhang, R., 2007. Large fluctuations of dissolved oxygen in the Indian and Pacific oceans during Dansgaard-Oeschger oscillations caused by variations of North Atlantic Deep Water subduction. Paleoceanography 22, PA3207. doi:10.1029/2006PA001384.
Schott, F.A., Xie, S.P., McCreary Jr., J.P., 2009. Indian Ocean circulation and climate variability. Rev. Geophys 47, RG1002. doi:10.1029/2007RG000245.
Schulz, H., von Rad, U., Ittekkot, V., 2002. Planktic foraminifera, particle flux and oceanic productivity off Pakistan, NE Arabian Sea: modern analogues and application to the palaeoclimatic record. Geological Society, 195. Special Publications, London, pp. 499–516. doi:10.1144/GSL.SP.2002.195.01.27.
Sirocko, F., Sarnthein, M., Lange, H., Erlenkeuser, H., 1991. Atmospheric summer circulation and coastal upwelling in the Arabian Sea during the Holocene and the last glaciation. Quat. Res. 36 (1), 72–93.
Sirocko, F., Garbe-Schonberg, D., Devey, C., 2000. Processes controlling trace element geochemistry of Arabian Sea sediments during the last 25,000 years. Glob. Planet. Chang. 26 (1–3), 217–303.
Stuiver, M., Reimer, P.J., Bard, E., Beck, J.W., Burr, G.S., Hughen, K.A., Kromer, B., McCormac, G., Van Der Plicht, J., Spurk, M., 1998. INTCAL98 radiocarbon age calibration, 24,000-0 cal BP. Radiocarbon 40, 1041–1083.
von Rad, U., Schulz, H., Sonne 90 Scientific Party1, Ali Khan, A., Ansari, M., Berner, U., Čepek, P., Cowie, G., Dietrich, P., Erlenkeuser, H., Geyh, M., Jennerjahn, T., Lückge, A., Marchig, V., Riech, V., Rösch, H., Schäfer, P., Schulte, S., Sirocko, F., Tahir, M., Weiss, W., 1995. Sampling the oxygen minimum zone off Pakistan: glacial–interglacial variations of anoxia and productivity (preliminary results, sonne 90 cruise). Mar. Geol. 125, 7–19.
von Rad, U., Schaaf, M., Michels, K.H., Schulzc, H., Bergerd, W.H., Sirocko, F., 1999. A 5000-yr record of climate change in varved sediments from the oxygen minimum zone off Pakistan, Northeastern Arabian Sea. Quat. Res. 51, 39–53.
Waelbroeck, C., Labeyrie, L., Michel, E., Duplessy, J.C., McManus, J.F., Lambeck, K., Balbon, E., Labracherie, M., 2002. Sea-level and deep water temperature changes derived from benthic foraminifera isotopic records. Quat. Sci. Rev. 21, 295–305.
Wang, Y.J., Cheng, H., Edwards, R.L., An, Z.S., Wu, J.Y., Shen, C.C., Dorale, J.A., 2001. A high-resolution absolute-dated late Pleistocene monsoon record from Hulu Cave, China. Science 294, 2345.
Wang, Y., Cheng, H., Edwards, R.L., Kong, X., Shao, X., Chen, S., Wu, J., Jiang, X., Wang, X., An, Z., 2008. Millennial- and orbital-scale changes in the East Asian monsoon over the past 224,000 years. Nature 451, 1090–1093.
Weyhenmeyer, C.E., Burns, S.J., Waber, H.N., Aeschbach-Hertig, W., Kipfer, R., Loosli, H.H., Matter, A., 2000. Cool glacial temperatures and changes in moisture source recorded in Oman groundwaters. Science 287. doi:10.1126/science.287.5454.842.
You, Y., 1998. Intermediate water circulation and ventilation of the Indian Ocean derived from water-mass contributions. J. Mar. Res. 56, 1029–1067. doi:10.1357/002224098765173455.
Yu, E.F., François, R., Bacon, M.P., 1996. Similar rates of modern and last-glacial ocean thermohaline circulation inferred from radiochemical data. Nature 379, 689–694.
Zaragosi, S., Bourillet, J.F., Eynaud, F., Toucanne, S., Denhard, B., Van Toer, A., Lanfumey, V., 2006. The impact of the last European deglaciation on the deep-sea turbidite systems of the Celtic-Armorican margin (Bay of Biscay). Geo-Mar. Lett. 26, 317–329.
Ziegler, M., Jilbert, T., de Lange, G.J., Lourens, L.J., Reichart, G.J., 2008. Bromine counts from XRF scanning as an estimate of the marine organic carbon content of sediment cores. Geochem. Geophys. Geosyst. 9, Q05009. doi:10.1029/2007GC001932.
Ziegler, M., Lourens, L.J., Tuenter, E., Hilgen, F., Reichart, G.J., Weber, N., 2010a. Precession phasing offset between Indian summer monsoon and Arabian Sea productivity linked to changes in Atlantic overturning circulation. Paleoceanography 25, PA3213. doi:10.1029/2009PA001884.
Ziegler, M., Tuenter, E., Lourens, L.J., 2010b. The precession phase of the boreal summer monsoon as viewed from the eastern Mediterranean (ODP Site 968). Quat. Sci. Rev. 29. doi:10.1016/j.quascirev.2010.03.011.
Ziegler, M., Lourens, L.J., Tuenter, E., Reichart, G.J., 2010c. High Arabian Sea productivity conditions during MIS 13—odd monsoon event or intensified overturning circulation at the end of the Mid-Pleistocene transition? Clim. Past 6, 63–76.